NUCLEAR PHYSICS

Original article
DOI: https://doi.org/10.18721/JPM.18211

# FEASIBILITY TO MEASURE THE PROPERTIES OF CHARGED *K**(892) MESONS AND Σ(1385) BARYONS IN COLLISIONS OF BISMUTH NUCLEI AT AN ENERGY OF 9.2 GeV IN THE NICA COLLIDER USING THE MPD EXPERIMENTAL SETUP

*Ya. A. Berdnikov*[1], *D. A. Ivanishchev*[1]✉, *D. O. Kotov*[1], *M. V. Malaev*[1], *A. Yu. Riabov*[2]

[1] Peter the Great St. Petersburg Polytechnic University, St. Petersburg, Russia;

[2] Petersburg Nuclear Physics Institute named after B. P. Konstantinov of NRC Kurchatov Institute, St. Petersburg, Russia

✉ ivanishchev_da@pnpi.nrcki.ru

**Abstract.** We report results on a feasibility study of measuring the properties of $K^*(892)^\pm$ and $\Sigma(1385)^\pm$ resonances in collisions of bismuth nuclei (Bi) at an energy of 9.2 GeV using the MPD detector at the NICA collider. The dependencies of the processes key parameters on the transverse momentum for different intervals of centrality of Bi + Bi collisions were obtained in the rapidity range from −0.5 to +0.5 using model calculations. The evaluations of the mass resolution, detection efficiency of the MPD detector and the transverse momentum spectra for the $K^*(892)^\pm$ and $\Sigma(1385)^\pm$ resonances were made. The sample size of Bi + Bi collision data that allowed the $K^*(892)^\pm$ and $\Sigma(1385)^\pm$ resonances properties to be reconstructed with a sufficiently good accuracy to conduct a study of the $K^*(892)^\pm$ and $\Sigma(1385)^\pm$ resonances production was estimated.

**Keywords:** bismuth nuclei collisions, production, resonance, NICA collider, MPD detector

**Funding:** The reported study was carried out within the framework of the State Assignment for Fundamental Research (Subject Code FSEG-2025-0009).

**Citation:** Berdnikov Ya. A., Ivanishchev D. A., Kotov D. O., Malaev M. V., Riabov A. Yu., Feasibility to measure the properties of charged K*(892) mesons and Σ(1385) baryons in collisions of bismuth nuclei at an energy of 9.2 GeV in the NICA collider using the MPD experimental setup, St. Petersburg State Polytechnical University Journal. Physics and Mathematics. 18 (2) (2025) 119–131. DOI: https://doi.org/10.18721/JPM.18211

This is an open access article under the CC BY-NC 4.0 license (https://creativecommons.org/licenses/by-nc/4.0/)

© Berdnikov Ya. A., Ivanishchev D. A., Kotov D. O., Malaev M. V., Riabov A. Yu., 2025. Published by Peter the Great St. Petersburg Polytechnic University.

Научная статья
УДК 539.126.3, 539.126.6
DOI: https://doi.org/10.18721/JPM.18211

# ВОЗМОЖНОСТИ ИЗМЕРЯТЬ СВОЙСТВА ЗАРЯЖЕННЫХ $K^*$(892)-МЕЗОНОВ И $\Sigma$(1385)-БАРИОНОВ В СТОЛКНОВЕНИЯХ ЯДЕР ВИСМУТА ПРИ ЭНЕРГИИ 9,2 ГэВ В УСКОРИТЕЛЕ NICA НА ЭКСПЕРИМЕНТАЛЬНОЙ УСТАНОВКЕ MPD

*Я. А. Бердников*[1], *Д. А. Иванищев*[1]✉, *Д. О. Котов*[1], *М. В. Малаев*[1], *А. Ю. Рябов*[2]

[1] Санкт-Петербургский политехнический университет Петра Великого, Санкт-Петербург, Россия;

[2] Петербургский институт ядерной физики им. Б. П. Константинова

НИЦ «Курчатовский институт», Санкт-Петербург, Россия

✉ ivanishchev_da@pnpi.nrcki.ru

**Аннотация.** В статье представлены результаты исследования возможности измерять свойства $K^*(892)^\pm$- и $\Sigma(1385)^\pm$-резонансов в столкновениях ядер висмута Bi при энергии 9,2 ГэВ с помощью экспериментальной установки (ЭУ) MPD на ускорителе NICA. Прослежены зависимости ключевых параметров процессов от поперечного импульса для различных интервалов по центральности столкновений Bi + Bi в области быстрот от −0,5 до 0,5+ посредством модельных расчетов. Получены оценки массового разрешения ЭУ MPD, эффективности регистрации в ЭУ MPD и спектров по поперечному импульсу для $K^*(892)^\pm$- и $\Sigma(1385)^\pm$-резонансов. Проведена оценка объема выборки данных (Bi + Bi)-столкновений, позволяющей восстановить свойства $K^*(892)^\pm$ и $\Sigma(1385)^\pm$ с достаточно хорошей точностью для исследования рождения этих резонансов.

**Ключевые слова:** столкновение ядер висмута, рождение, резонанс, ускоритель NICA, детектор MPD

**Финансирование:** Работа выполнена в рамках Государственного задания на проведение фундаментальных исследований (код темы FSEG-2025-0009).

**Ссылка для цитирования:** Бердников Я. А., Иванищев Д. А., Котов Д. О., Малаев М. В., Рябов А. Ю. Возможности измерять свойства заряженных K*(892)-мезонов и Σ(1385)-барионов в столкновениях ядер висмута при энергии 9,2 ГэВ в ускорителе NICA на экспериментальной установке MPD // Научно-технические ведомости СПбГПУ. Физико-математические науки. 2025. Т. 18. № 2. С. 119–131. DOI: https://doi.org/10.18721/JPM.18211

Статья открытого доступа, распространяемая по лицензии CC BY-NC 4.0 (https://creativecommons.org/licenses/by-nc/4.0/)

## Introduction

One of the main goals of experiments on collisions of relativistic heavy nuclei is to construct a phase diagram of quantum chromodynamic (QCD) matter and to study the properties of such matter at high temperatures and baryon densities. Convincing evidence for production of strongly interacting quark-gluon plasma (QGP) has been obtained in collisions of heavy nuclei at energies achieved at the Relativistic Heavy Ion Collider (RHIC) at Brookhaven National Laboratory (BNL, USA), the Super Proton Synchrotron (SPS) and the Large Hadron Collider (LHC) at the European Organization for Nuclear Research (CERN, Switzerland) [1, 2].

© Бердников Я. А., Иванищев Д. А., Котов Д. О., Малаев М. В., Рябов А. Ю., 2025. Издатель: Санкт-Петербургский политехнический университет Петра Великого.

The evolution of the QGP is successfully described by hydrodynamic models assuming the presence of local thermal equilibrium and a number of specific initial conditions [3, 4]. The collision of relativistic heavy nuclei begins with primary nucleon-nucleon interactions. This is followed by the pre-equilibrium phase and production of QGP. As the system formed in collisions of relativistic heavy nuclei expands and cools, the process of hadronization begins, with the QGP subsequently transforming into colorless hadrons. Quarks and gluons are trapped inside hadrons. A dense and hot gas is produced from stable hadrons and resonances. The system reaches chemical freeze-out, at which inelastic collisions among hadrons cease, and the yields of stable particles are extracted [5].

After chemical freeze-out, the hadrons continue to interact with each other through elastic or pseudo-elastic (scattering through an intermediate state) scattering, exchanging momentum. The system reaches a stage when the mean free path of hadrons becomes significantly larger than the size of the system, i.e., the so-called kinetic freeze-out occurs. At this stage, a momentum distribution of hadrons is formed, their composition no longer changes and the hadrons move freely towards the detector devices. Since the temperatures of chemical freeze-out and the quark-hadron transition are close to each other, the phase between chemical and kinetic freezing is called hadronic [6]. The late hadronic phase of collision between relativistic heavy nuclei is a unique medium for studying the hadron system at high temperatures and densities. Understanding the processes occurring in excited hadronic gas is of paramount importance for interpreting the observables used to characterize chemical and kinetic freeze-out, the hadronic phase, and, more broadly, the time evolution of a system formed in collisions of relativistic heavy ions. The properties of the hadronic phase are investigated by measuring hadron decays of short-lived resonances [7]. The lifetime $\tau$ of short-lived hadronic resonances is rather short and comparable to the duration of the hadronic phase (about 10 fm/*c* [8]). In this context, short-lived hadronic resonances are sensitive probes for studying the hadronic phase. Hadronic resonances with the shortest lifetime, such as $\rho(770)$ meson ($\tau \approx 1$ fm/*c* [9]), decay during the hadronic phase. Their daughter particles can be scattered by the surrounding hadrons in dense hadronic matter, changing the momentum and direction of motion. As a result, the initial information about the resonance from which they originated is lost.

Due to the lack of correlation between the daughter particles, the resonance cannot be reconstructed by the standard invariant mass analysis, and the measured yield appears to be suppressed compared to the expected value [8]. Other observables of the resonances also change, such as the shape of the transverse momentum spectrum, mass, width, etc. The situation is further complicated by recombination effects, where hadrons in the hadronic gas recombine to produce new resonances, leading to an increase in the yield compared to its initial value. The intensity of these two processes depends on the lifetime of the hadronic phase, the density of the hadronic medium, the cross section of interactions between resonance decay products and other hadrons, and the lifetime of the resonances themselves.

The predominance of one effect over another can be investigated by studying the ratio of the resonance yields to the yields of long-lived hadrons with the same quark composition as a function of collision centrality. Hadronic resonances with a long lifetime, such as the $\varphi(1020)$ meson ($\tau \approx 45$ fm/*c* [9]), most likely ‘survive’ the hadronic phase and decay in vacuum after kinetic freeze-out. This feature of such resonances is used for comparison with the production of shorter-lived resonances in reference measurements [10].

In addition to different lifetimes, hadronic resonances have different quark composition, mass, baryon number and strangeness. Therefore, comprehensive analysis of resonance production allows to understand not only the properties of the hadronic phase and its evolution, but also other effects peculiar to dense and hot nuclear matter. These are, for example, the mechanisms of hadronization in the region of intermediate and large transverse momenta, the dynamics of processes and reactions forming the transverse momentum spectra of particles, the excess yield of baryons relative to mesons, the excess yield of strangeness, etc. [10]. Hadronic resonances are produced in sufficient numbers. Daughter particles of their hadronic decays can be detected using detector setups, and their properties can be easily reconstructed by the invariant mass method even for cascade resonance decays.

The following resonances with dominant hadronic cascade decays play a special role for systematic study of hadronic resonances [9]:

| Elementary particle | Lifetime $\tau$, fm/$c$ |
|---|---|
| $\Sigma(1385)^-$ baryon | $\approx$ 5.01, |
| $\Sigma(1385)^+$ baryon | $\approx$ 5.45, |
| $K^*(892)^+$ meson | $\approx$ 3.84, |
| $K^*(892)^-$ meson | $\approx$ 3.83. |

These resonances have lifetimes comparable to the lifetime of the hadronic phase. Similar to $K^*(892)^0$ and $\rho(770)$ mesons, they decay during the hadronic phase. Depending on the pree dominance of rescattering or recombination effects, their yield may be suppressed or excessive, compared with the reference measurements of the yield of quasi-stable particles with a similar quark composition. Experimental observation of the predominance of a specific effect for a wide range of resonances allows to more accurately define the cross sections of hadronic interactions to describe the known hadronic processes for simulation of the hadronic phase.

The quark compositions of $\Sigma(1385)^-$-($uss$), $\Sigma(1385)^+$-($dds$) baryons as well as $K^*(892)^+$-($s\bar{u}$) and $K^*(892)^-$-($u\bar{s}$) mesons include strange quarks; unlike the $\varphi$ meson, they are open-strange. This property of these resonances allows to explore the production of strangeness more comprehensively by measuring their production together with the production of $\varphi$ mesons. The different number of quarks included in the resonances under consideration also makes it possible to use them to study the excess yield of baryons relative to mesons, the mechanisms of hadronization, etc.

In the near future, after the Nuclotron-based Ion Collider (NICA) at the Joint Institute for Nuclear Research ( Dubna, Russia) is commissioned, an experiment on studying the processes during collisions of heavy nuclei (Multi-Purpose Detector (MPD)) will begin at the collider facility [11]. It is expected that the first colliding systems at the NICA will be the nuclei of bismuth (Bi + Bi) and xenon (Xe + Xe) atoms at a center-of-mass energy (per nucleon pair) $\sqrt{S_{NN}}$ = 7.0–9.2 GeV.

Systematic study of the production of resonances in collisions of relativistic nuclei at the energy of NICA is one of the main objectives of the MPD experiment, continuing the research on the production of resonances at the SPS, RHIC and LHC accelerators.

Preparations are currently underway for the launch of the collider facility. Measurement techniques are developed and potential observables are estimated based on model calculations. Special attention is paid to the development of complex algorithms, validated based on model calculations.

The goal of this study is to determine the possibility of measuring the properties of hadronic resonances of $\Sigma(1385)^-$ and $\Sigma(1385)^+$baryons as well as $K^*(892)^+$-($su$) and $K^*(892)^-$-($u\bar{s}$) mesons using the MPD setup in the NICA accelerator in collisions of bismuth nuclei at $\sqrt{S_{NN}}$ = 9.2 GeV in hadron cascade decay channels

$$\Sigma(1385)^- \to \Lambda + \pi^-,$$

$$\Sigma(1385)^+ \to \Lambda + \pi^+ \ (\Lambda \to p + \pi^-),$$

$$K^*(892)^+ \to K_S + \pi^+,$$

$$K^*(892)^- \to K_S + \pi^- (K_S \to \pi^+ + \pi^-)$$

in the rapidity range $|y| < 0.5$ and depending on the collision centrality.

## Experimental setup of the MPD and computational procedure

This facility is one of the two large detector systems at the NICA accelerator, optimized for studying dense and hot matter formed in collisions of relativistic heavy ions. The facility includes a central part, which has a large time projection chamber, a time-of-flight detector and an electromagnetic calorimeter (located inside a superconducting solenoid). Detectors are connected to the central part from the front and back, which are used to select events, measure the vertex and time of interaction, as well as collision centrality of heavy ions. The most detailed information about the detectors of the experimental MPD setup, their parameters and efficiency evaluation can be found [11]. The paper describes the capabilities of the Time Projection Chamber (TPC) for reconstructing charged particle tracks and particle detection, as well as the Time-Of-Flight (TOF) detector for particle detection.

The MPD experiment, like the entire NICA facility, is under construction and is scheduled to be launched in the coming years. In view of this, efforts are underway to reliably simulate collisions of heavy ions at energies expected at the NICA accelerator in both the collider configuration and the configuration with fixed-target collisions. Detailed modeling of the responses of various detector subsystems included in the MPD experimental setup is also carried out in order to evaluate the capabilities of the experimental setup to recover signals from various kinds of physical processes that are supposed to be studied in the MPD experiment, in particular, those occurring during collisions of different systems at different collision energies.

In this paper, we analyze data obtained by simulating collisions of Bi nuclei at energy $\sqrt{S_{NN}}$ = 9.2 GeV. The UrQMD event generator, one of the most well-known and popular software packages for reliable simulation of heavy ion interactions in the energy range expected at the NICA accelerator, was used to simulate Bi + Bi collisions in a wide range of target parameter values. The studied resonances were declared stable particles in the input settings of the event generator.

Since the goal of this work was to explore the possibilities of a future MPD setup for reconstructing signals from cascade resonance decays, this setting was used to minimize distortion of the results obtained. The distortions are caused by the effects of the late hadronic phase in the interaction of heavy relativistic ions (rescattering and regeneration of daughter particles in hadronic gas). The simulated (Bi + Bi) collision events obtained by the UrQMD generator were then used to simulate the response of the MPD using the MpdRoot software package [11]. This package serves as the main tool for both simulating and processing the results obtained by the MPD setup. It contains the most up-to-date, accurate and detailed geometry of all detector subsystems, described using the GEANT software package, as well as tools for reconstructing charged particle tracks, signal processing of electromagnetic and hadronic calorimeters, particle detection, etc. The MpdRoot package was also applied to simulate the decay of the studied resonances in accordance with their tabulated parameters using the GEANT software package [9].

In this paper, we studied the decays of the following resonances in cascade modes (with the presence of a secondary vertex):

$$K^*(892)^{\pm} \rightarrow K_S + \pi^{\pm} \ (K_S \rightarrow \pi^+ + \pi^-),$$

$$\Sigma(1385)^{\pm} \rightarrow \Lambda + \pi^{\pm} \ (\Lambda \rightarrow p + \pi^-).$$

Analysis of such decays is peculiar in that the secondary vertex of the decay of $K_S$ mesons and $\Lambda$ baryons must be reconstructed before reconstructing the signal from the decay of the studied resonance. Since the inner tracking system will not be assembled at the first stage of experiments with the MPD setup (in the future it will allow more accurate reconstruction of secondary vertices), this study was aimed at optimizing the selection of candidates (by the required criteria) for secondary vertex from the decay of $K_S$ mesons and $\Lambda$ baryons (in particular, using tools from the MpdRoot software package). It was necessary to minimize the background level in the resulting distributions without significant loss of useful signal. More efficient algorithms were used for reconstructing charged particle tracks, and the data sample for (Bi + Bi) collisions was increased to 50 million collisions, compared with those described in [12, 13] (where it was 5 million), considering the capabilities of the MPD setup for measuring the properties of $K^*(892)^{\pm}$ and $\Sigma(1385)^{\pm}$ resonances in (Au + Au) collisions at energies $\sqrt{S_{NN}}$ = 4.0, 7.7 and 11.0 GeV [12] and Bi + Bi collisions at energies $\sqrt{S_{NN}}$ = 9.2 GeV [13]. In addition, the detector subsystems of the MPD setup were described in more detail based on new information.

Thanks to the application of new optimized algorithms and a larger-scale study, we obtained for the first time new interesting results reflecting the dependence on the collision centrality (which is the most important).

The properties of $K^*(892)^+$ and $K^*(892)^-$ resonances as well as $\Sigma(1385)^+$ and $\Sigma(1385)^-$ resonances are close, while their hadronic decays differ by the pion charge. This paper considered averaged sums to expand statistics and facilitate the reconstruction of the properties of the studied resonances.

$$[K^*(892)^+ + K^*(892)^-]/2 \text{ and } [\Sigma(1385)^+ + \Sigma(1385)^-]/2.$$

Events with a reconstructed interaction vertex within 130 cm along the $z$ axis from the geometric center of the experimental setup were selected from the total sample. This requirement is imposed because constant trigger efficiency must be maintained along the $z$-coordinate of the interaction vertex. We estimated the centrality of events based on information about the multiplicity of charged particles reconstructed in the TPC detector [10].

A comprehensive technique was developed and improved to reconstruct the signal from the decays of the studied resonances taking into account the topology of the decays, the parameters and capabilities of the MPD, as well as possible background processes distorting the reconstructed signal. For each event, all the analyzed tracks of charged particles were tested for several criteria to select the tracks to be used to reconstruct the signal from the decays of the studied resonances. All tracks should be identified either as pions or as protons (depending on which type of particles were selected at this stage) using information from the TPC and TOF detectors. Only the most accurately reconstructed tracks were considered for selection; the selection criteria used were the minimal number of points in the TPC used to reconstruct the track and the maximum pseudorapidity of the reconstructed charged particle track.

To select pions from direct decay of $K^*(895)^\pm$ and $\Sigma(1385)^\pm$ resonances, the distance of the closest approach between the reconstructed track and the primary interaction vertex was also checked.

A separate stage was the selection of candidates and the reconstruction of the secondary decay vertex of $K_S$ mesons and $\Lambda$ baryons. In addition to the track selection criteria described above, the criterion of the minimal value of the parameter $\chi^2$ was used for the selection of pions (protons) for matching the reconstructed track to the primary vertex of the interaction. The tracks selected in this way were combined into various $\pi^+\pi^-$ ($p\pi^-$) pairs in the case of reconstruction of the secondary vertex from the decay of $K_S$ mesons ($\Lambda$ baryons). Each analyzed pair was checked against the criteria for daughter particles from the decay of $K_S$ mesons or $\Lambda$ baryons:

maximum distance between two tracks at the secondary decay vertex;

reconstruction quality of the secondary vertex (maximum value of $\chi^2$);

minimum distance between the primary and secondary decay vertices;

maximum angle between the vector connecting the primary and secondary vertices and the vector of the reconstructed momentum of $K_S$ meson ($\Lambda$ baryon).

As a result, only pairs that passed all the selection criteria were used to reconstruct the invariant mass of the $\pi^+\pi^-$ ($p\pi^-$) pair to isolate the signal from the decay of $K_S$ mesons ($\Lambda$ baryons).

Fig. 1 shows examples of the distributions of the reconstructed invariant masses for $\pi^+\pi^-$ and $p\pi^-$ pairs before and after applying the selection criteria. Evidently, applying these selection criteria significantly suppresses the background component of the distributions, which makes it possible to isolate signals with minimal background fraction from the decays of $K_S$ mesons and $\Lambda$ baryons for further analysis.

For the purpose of further analysis, candidates for decay of $K_S$ mesons and $\Lambda$ baryons in the range of $\pm 2$ standard deviations from the tabulated mass of the $K_S$ meson or $\Lambda$ baryon were selected from the distributions shown in Fig. 1, *b*, *d*. Candidates for $K_S$ mesons ($\Lambda$-baryons) selected in this way were combined with charged pions that passed all the selection criteria, generating the distributions of invariant masses for $\pi K_S$ ($\pi\Lambda$) pairs. The obtained distributions contained, in addition to the signal from the decays of the studied resonances, a significant combinatorial background, which was evaluated by the event mixing method. Close values of the $z$-coordinate of the collision vertex position and the multiplicity of reconstructed event particles were selected for each analyzed event to evaluate the combinatorial background. The method described above was used to reconstruct the invariant mass of $\pi K_S$ ($\pi\Lambda$) pairs, however, the pions for this pair were taken from the analyzed event, and candidates for $K_S$ mesons ($\Lambda$ baryons) were taken from selected similar events. The distribution of invariant masses obtained by event mixing was normalized by the analyzed distribution in the invariant mass region, where no useful signal was expected; then this distribution was subtracted from the analyzed distribution. Fig. 2 shows examples of the distributions of invariant masses for of $\pi K_S$ and $\pi\Lambda$ pairs before and after subtracting the combinatorial background.

The distribution formed after subtracting the combinatorial background was fitted to a composite function to calculate the yields of $K^*(892)^\pm$ and $\Sigma(1385)^\pm$ resonances in (Bi + Bi) collisions at $\sqrt{S_{NN}}$ = 9.2 GeV, obtained after applying all selection criteria.

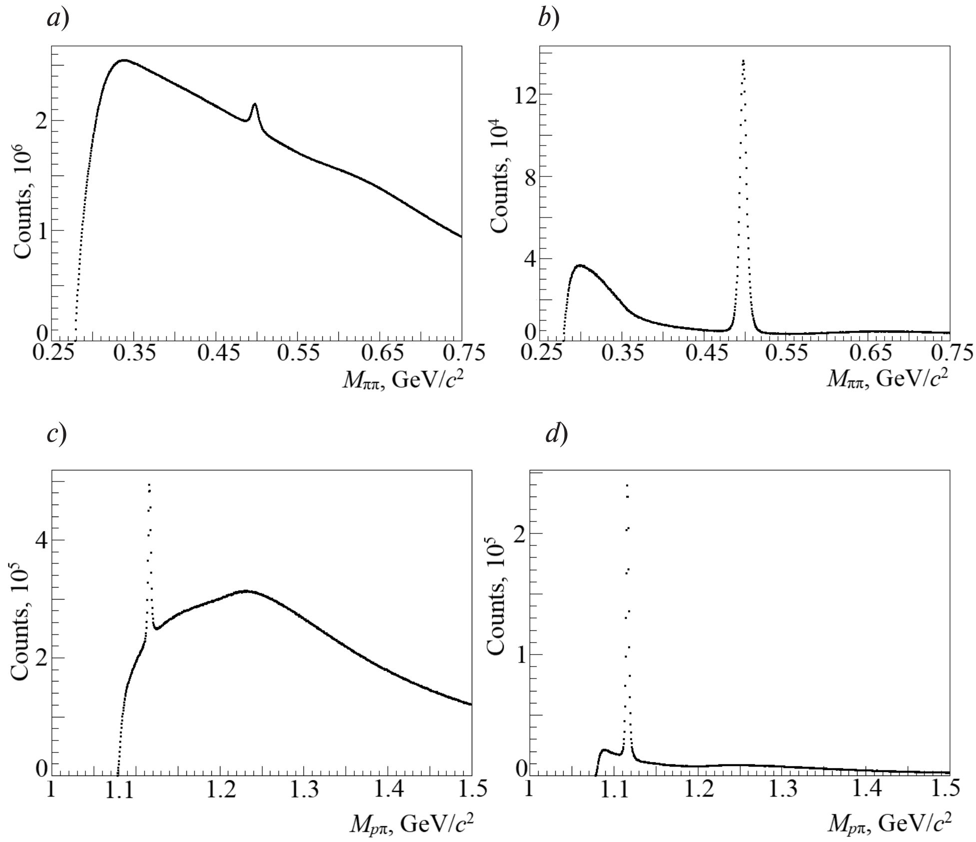


Fig. 1. Invariant mass spectra for pair of oppositely charged pions $\pi\pi$ (*a*, *b*) and proton-$\pi^-$ pair (*c*, *d*) in collisions of bismuth (Bi + Bi) nuclei at $\sqrt{S_{NN}}$ = 9.2 GeV before (*a*, *c*) and after (*b*, *d*) applying the selection criteria Spectra were reconstructed in the transverse momentum range $0.4 < p_T < 0.6$ GeV/*c* for both pairs

The fitting function includes a convolution of the Breit–Wigner function (to describe the spectral shape of the resonance) and a Gaussian (to account for the mass resolution of the MPD), as well as a polynomial to account for the residual background. The integral of the Breit–Wigner function convolved with the Gaussian was taken as the yield.

The mass resolution for each analyzed transverse momentum range was estimated by constructing the distribution of the difference between the values of the generated and reconstructed mass of the studied resonance. This distribution was fitted to the Gaussian, and the width obtained from the fit was taken as the mass resolution [10]. Fig. 3 shows the dependences of mass resolution of the MPD setup on the transverse momentum value in the case of decay reconstruction.

$$K^*(892)^\pm \to K_S + \pi^\pm \ (a) \text{ and } \Sigma(1385)^\pm \to \Lambda + \pi^\pm \ (b).$$

Fig. 4 shows the distributions of decay reconstruction efficiency.

$$K^*(892)^\pm \to K_S + \pi^\pm \text{ and } \Sigma(1385)^\pm \to \Lambda + \pi^\pm \ (b)$$

in (Bi + Bi) collisions at $\sqrt{S_{NN}}$ = 9.2 GeV in different centrality bins. The distributions were obtained as a function of the transverse momentum value. Although the reconstruction efficiency is small at low transverse momenta in the case of $K^*(892)^\pm$ mesons, it still exceeds zero, while in the case of $\Sigma(1385)^\pm$ baryons, the efficiency drops to zero, imposing restrictions on the transverse momenta that are minimally achievable for signal reconstruction from baryon decays. As the transverse momentum increases, the reconstruction efficiencies of $K^*(892)^\pm$ and $\Sigma(1385)^\pm$resonances increase, reaching a value of 0.2, after which they remain stable. This means that the maximum achievable values of the transverse momentum are limited only by the statistical sample collected.

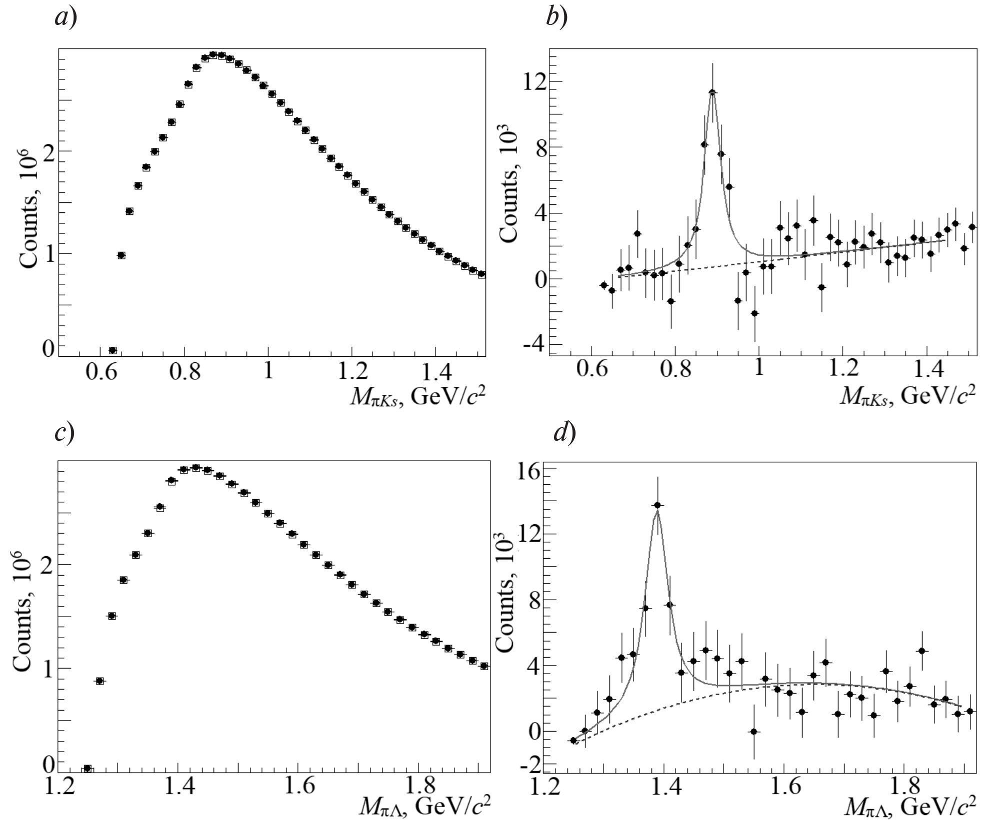


Fig. 2. Invariant mass spectra for $\pi K_S$($a$, $b$) and $\pi\Lambda$ ($c$, $d$) pairs (black symbols) in (Bi + Bi) collisions at $\sqrt{S_{NN}}$ = 9.2 GeV before ($a$, $c$) and after ($b$, $d$) subtraction of the combinatorial background (squares).
Spectra were reconstructed in the transverse momentum ranges $0.4 < p_T^{\pi Ks} < 0.6$ GeV/$c$ and $0.4 < p_T^{\pi\Lambda} < 0.6$ GeV/$c$ for $\pi K_S$ and $\pi\Lambda$ pairs, respectively
Breit–Wigner function convolved with a Gaussian is used to reconstruct the peak (solid line); second-degree polynomial is used for the correlated background (dashed line)

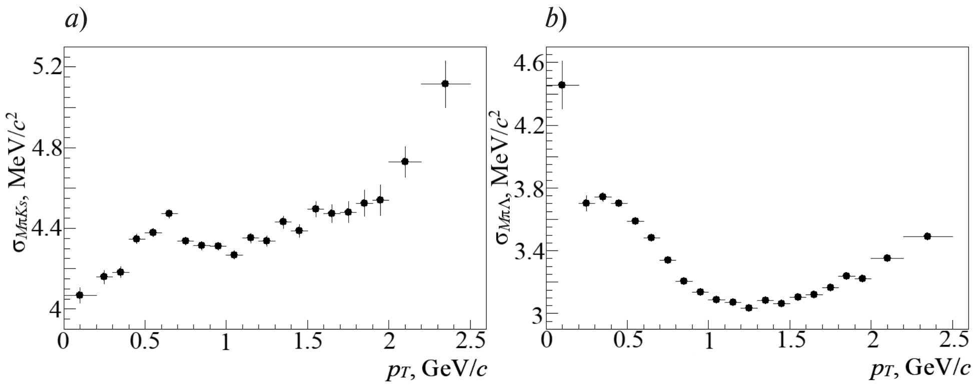


Fig. 3. Dependences of mass resolution of MPD ($\sigma_{M\pi Ks}$ and $\sigma_{M\pi\Lambda}$) on transverse momentum $p_T$ of $\pi K_S$ ($a$) and $\pi\Lambda$ ($b$) pairs for $K^*(892)^\pm \to K_S + \pi^\pm$ ($a$) and $\Sigma(1385)^\pm \to \Lambda + \pi^\pm$ ($b$) decay channels in (Bi + Bi) collisions at $\sqrt{S_{NN}}$ = 9.2 GeV

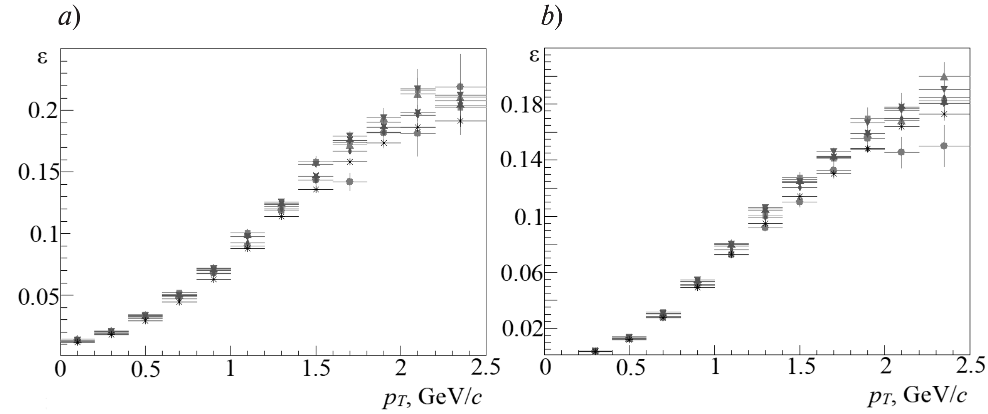


Fig. 4. Dependences of detection efficiency ε for $K^*(892)^{\pm}$ and $\Sigma(1385)^{\pm}$ resonances on transverse momentum in $K^*(892)^{\pm} \rightarrow K_S + \pi^{\pm}$ (*a*) and $\Sigma(1385)^{\pm} \rightarrow \Lambda + \pi^{\pm}$ (*b*) decay channels, extracted using MPD

Efficiency was calculated for (Bi + Bi) collisions at $\sqrt{S_{NN}}$ = 9.2 GeV for 7 centrality bins, %: 0–10 (∗), 10–20 (♦), 20–30 (⋆), 30–40 (▼), 40–50 (▲), 50–60 (■) and 60–90(•)

**Computational results**

To construct the dependence of invariant yields on the transverse momentum (the so-called transverse momentum spectrum), the differential yields were calculated for each of the considered transverse momentum ranges and centrality bins of (Bi + Bi) collisions using the following formula [10]:

$$\frac{d^2N}{dp_T dy} = \frac{N(p_T)}{N_{\mathrm{ev}}\varepsilon(p_T)\Delta p_T \Delta y}, \quad (1)$$

where $N(p_T)$ are the yields of $K^*(892)^{\pm}$- and $\Sigma(1385)^{\pm}$-resonances; $N_{ev}$ is the number of collisions analyzed; $p_T$, GeV/c, is the transverse momentum of $K^*(892)^{\pm}$- and $\Sigma(1385)^{\pm}$-resonances; $\Delta p_T$, GeV/*c*, is the transverse momentum range within which the yields of these resonances are determined; $\Delta y$ is the rapidity range from −0.5 до 0.5; $\varepsilon(p_T)$ is the detection efficiency of $K^*(892)^{\pm}$- and $\Sigma(1385)^{\pm}$-resonances, equal to the geometric acceptance of the MPD for the studied hadronic resonance decays multiplied by the average decay probabilities for each channel

$$K^*(892)^{\pm} \rightarrow K_S + \pi^{\pm} \text{ and } \Sigma(1385)^{\pm} \rightarrow \Lambda + \pi^{\pm}.$$

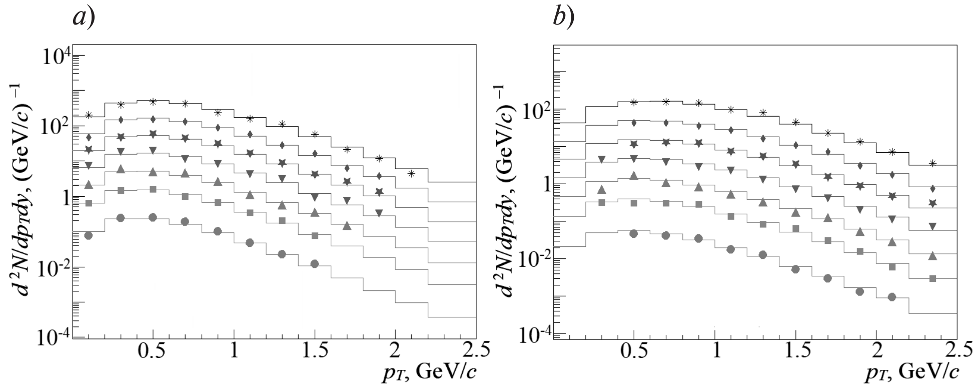


Fig. 5. Reconstructed transverse momentum spectra (symbols) and similar spectra initially generated by event generator (lines) for $K^*(892)^{\pm}$ (*a*) and $\Sigma(1385)^{\pm}$ (*b*) resonances in the rapidity range $|y| < 0.5$

These data correspond to the same collisions and energies, for the same centrality bins and notations as in Fig. 4. For clarity, the enlarged spectra are shown in one graph

The transverse momentum spectra for $K^*(892)^\pm$ and $\Sigma(1385)^\pm$ resonances are shown in Fig. 5. The spectra were obtained for various centrality bins of (Bi + Bi) collisions at $\sqrt{S_{NN}}$ = 9.2 GeV in the rapidity range $|y| < 0.5$. The real transverse momentum spectra of $K^*(892)^\pm$- and $\Sigma(1385)^\pm$ resonances generated by the event generator are also shown for comparison. Evidently, the spectra are similar, which confirms the adequacy of the analytical procedure we developed. It can also be seen from the obtained transverse momentum spectra that for measuring the properties of $K^*(892)^\pm$ and $\Sigma(1385)^\pm$ resonances in hadron cascade decay channels

$$K^*(892)^\pm \rightarrow K_S + \pi^\pm \text{ and } \Sigma(1385)^\pm \rightarrow \Lambda + \pi^\pm,$$

depending on the transverse momentum and collision centrality, a sample exceeding 50 million (Bi + Bi) collisions is sufficient.

## Conclusion

The paper reports on the feasibility of measuring the properties of $K^*(892)^\pm$ and $\Sigma(1385)^\pm$ resonances in collisions of bismuth nuclei at energy $\sqrt{S_{NN}}$ = 9.2 GeV at the MPD experimental facility that is part of the NICA accelerator complex. The study was performed by simulating the collisions of bismuth nuclei and reconstructing the following hadronic cascade decays:

$$\Sigma(1385)^- \rightarrow \Lambda + \pi^-,$$

$$\Sigma(1385)^+ \rightarrow \Lambda + \pi^+ \ (\Lambda \rightarrow p + \pi^-),$$

$$K^*(892)^+ \rightarrow K_S + \pi^+,$$

$$K^*(892)^- \rightarrow K_S + \pi^- (K_S \rightarrow \pi^+ + \pi^-).$$

The dependences of the main process parameters on the transverse momentum were obtained in these decays, for various centrality bins of (Bi + Bi) collisions in the rapidity range from −0.5 to 0.5. It was established that the accumulation of over 50 million of these collisions is sufficient for reconstructing the properties of $K^*(892)^\pm$ and $\Sigma(1385)^\pm$ resonances with satisfactory accuracy to study the production of $K^*(892)^\pm$ and $\Sigma(1385)^\pm$resonances in a wide range of transverse momenta: from 0 for $K^*(892)^\pm$ mesons and from 0.2 for $\Sigma(1385)^\pm$ baryons to 2.5 GeV/$c$ for both resonances and centralities of (Bi + Bi) collisions with a 10% bin for central and semi-central collisions, as well as with a 30% bin for peripheral ones.

## REFERENCES

1. **Adcox K., Adler S. S., Afanasiev S. V., et al.** (PHENIX Collaboration), Formation of dense partonic matter in relativistic nucleus–nucleus collisions at RHIC: Experimental evaluation by the PHENIX Collaboration, Nucl. Phys. A. 757 (1–2) (2005) 184 – 283.

2. **Aamodt K., Abelev B., Quintana A. A., et al.** (ALICE Collaboration), Higher harmonic anisotropic flow measurements of charged particles in Pb-Pb collisions at $\sqrt{S_{NN}}$ = 2.76 TeV, Phys. Rev. Lett. 107 (3) (2011) 032301.

3. **Schenke B., Shen C., Tribedy P.,** Hybrid color glass condensate and hydrodynamic description of the relativistic heavy ion collider small system scan, Phys. Lett. B. 803 (10 April) (2020) 135322.

4. **Andronic A., Braun-Munzinger P., Redlich K., Stachel J.,** Decoding the phase structure of QCD via particle production at high energy, Nature. 561 (7723) (2018) 321 – 330.

5. **Heinz U. W., Kestin G.,** Jozso's legacy: Chemical and kinetic freeze-out in heavy-ion collisions. Eur. Phys. J. Spec. Top. 155 (1) (2008) 75 – 87.

6. **Steinheimer J., Aichelin J., Bleicher M., Stцcker H.,** Influence of the hadronic phase on observables in ultrarelativistic heavy ion collisions, Phys. Rev. C. 95 (6) (2017) 064902.

7. **Riabov V.,** Short-lived resonances as probes of the medium produced in heavy-ion collisions, Particles. 4 (1) (2021) 1–10.

8. **Acharya S., Adamovб D., Adler A., et al.** (ALICE Collaboration), Evidence of rescattering effect in Pb–Pb collisions at the LHC through production of $K^*(892)^0$ and $\phi(1020)$ mesons, Phys. Lett. B. 802 (10 March) (2020) 135225.

9. **Workman R. L., Burkert V. D., Crede V., et al.** (Particle Data Group and Others), Review of particle physics, Prog. Theor. Exp. Phys. 2022 (8) (2022) 083C01.

10. **Berdnikov Ya. A., Ivanishchev D. A., Kotov D. O., et al.,** Feasibility to measure the properties of φ(1020) meson in collisions of bismuth nuclei at an energy of 9.2 GeV in the NICA collider using the MPD experimental setup, St. Petersburg State Polytechnical University Journal. Physics and Mathematics. 18 (1) (2025) 129–141. (in Russian).

11. **Abgaryan V., Acevedo Kado R., Afanasyev S. V., et al.,** Status and initial physics performance studies of the MPD experiment at NICA, Eur. Phys. J. A. 58 (7) (2022) 140.

12. **Ivanishchev D., Kotov D., Malaev M., et al.,** Resonance reconstruction in the MPD, Particles. 4 (1) (2021) 29–36.

13. **Ivanishchev D. A., Kotov D. O., Kryshen E. L., et al.,** Hadronic resonances as probes of late hadronic phase in heavy-ion collisions at NICA energies, PEPAN. 54 (3) (2023) 461–472.

## СПИСОК ЛИТЕРАТУРЫ

1. **Adcox K., Adler S. S., Afanasiev S., et al.** (PHENIX Collaboration). Formation of dense partonic matter in relativistic nucleus–nucleus collisions at RHIC: Experimental evaluation by the PHENIX Collaboration // Nuclear Physics A. 2005. Vol. 757. No. 1–2. Pp. 184 – 283.

2. **Aamodt K., Abelev B., Quintana A. A., et al.** (ALICE Collaboration). Higher harmonic anisotroɵpic flow measurements of charged particles in Pb-Pb collisions at $\sqrt{S_{NN}}$ = 2.76 TeV // Physical Review Letters. 2011. Vol. 107. No. 3. P. 032301.

3. **Schenke B., Shen C., Tribedy P.** Hybrid color glass condensate and hydrodynamic description of the relativistic heavy ion collider small system scan // Physics Letters B. 2020. Vol. 803 (10 April) P. 135322.

4. **Andronic A., Braun-Munzinger P., Redlich K., Stachel J.** Decoding the phase structure of QCD via particle production at high energy // Nature. 2018. Vol. 561. No. 7723. Pp. 321 – 330.

5. **Heinz U. W., Kestin G.** Jozso's legacy: Chemical and kinetic freeze-out in heavy-ion collisions // The European Physical Journal Special Topics. 2008. Vol. 155. No. 1. Pp. 75 – 87.

6. **Steinheimer J., Aichelin J., Bleicher M., Stцcker H.** Influence of the hadronic phase on observables in ultrarelativistic heavy ion collisions // Physical Review C. 2017. Vol. 95. No. 6. P. 064902.

7. **Riabov V.** Short-lived resonances as probes of the medium produced in heavy-ion collisions // Particles. 2021. Vol. 4. No. 1. Pp. 1–10.

8. **Acharya S., Adamovб D., Adler A., et al.** (ALICE Collaboration). Evidence of rescattering effect in Pb–Pb collisions at the LHC through production of $K^*(892)^0$ and ϕ(1020) mesons // Physics Letters B. 2020. Vol. 802 (10 March) P. 135225.

9. **Workman R. L., Burkert V. D., Crede V., et al.** (Particle Data Group and Others). Review of particle physics // Progress of Theoretical and Experimental Physics. 2022. Vol. 2022. No. 8. P. 083C01.

10. **Бердников Я. А., Иванищев Д. А., Котов Д. О., Малаев М. В., Рябов А. Ю.** Возможности измерять свойства φ(1020)-мезона в столкновениях ядер висмута при энергии 9,2 ГэВ в ускорителе NICA на экспериментальной установке MPD // Научно-технические ведомости СПбГПУ. Физико-математические науки. 2025. Т. 18. № 1. С. 129–141.

11. **Abgaryan V., Acevedo Kado R., Afanasyev S. V., et al.** Status and initial physics performance studies of the MPD experiment at NICA // The European Physical Journal A. 2022. Vol. 58. No. 7. P. 140.

12. **Ivanishchev D., Kotov D., Malaev M., Riabov V., Riabov Y.** Resonance reconstruction in the MPD // Particles. 2021. Vol. 4. No. 1. Pp. 29–36.

13. **Иванищев Д. А., Котов Д. О., Крышень Е. Л., Малаев М. В., Рябов В. Г., Рябов Ю. Г.** Адронные резонансы как пробники поздней адронной фазы в столкновениях тяжелых ионов при энергиях ускорителя NICA // Физика элементарных частиц и атомного ядра. 2023. Т. 54. № 3. С. 461–472.

## THE AUTHORS

**BERDNIKOV Yaroslav A.**
*Peter the Great St. Petersburg Polytechnic University*
29 Politechnicheskaya St., St. Petersburg, 195251, Russia
yberdnikov1947@gmail.com
ORCID: 0000-0003-0309-5917

**IVANISHCHEV Dmitry A.**
*Peter the Great St. Petersburg Polytechnic University*
29 Politechnicheskaya St., St. Petersburg, 195251, Russia
ivanishchev_da@pnpi.nrcki.ru
ORCID: 0000-0003-3298-3702

**KOTOV Dmitry O.**
*Peter the Great St. Petersburg Polytechnic University*
29 Politechnicheskaya St., St. Petersburg, 195251, Russia
Dmitriy.kotov@gmail.com
ORCID: 0000-0002-3395-0454

**MALAEV Mikhail V.**
*Peter the Great St. Petersburg Polytechnic University*
29 Politechnicheskaya St., St. Petersburg, 195251, Russia
Mmalayev@gmail.com
ORCID: 0009-0001-9974-0169

**RIABOV Andrei Yu.**
*Petersburg Nuclear Physics Institute named by B. P. Konstantinov of NRC "Kurchatov Institute"*
1, Orlova Roshcha (Mcr.), Gatchina, Leningrad Region, 188300, Russia
andrei.riabov@cern.ch
ORCID: 0009-0007-9874-9819

## СВЕДЕНИЯ ОБ АВТОРАХ

**БЕРДНИКОВ Ярослав Александрович** – *доктор физико-математических наук, профессор Высшей школы фундаментальных физических исследований Санкт-Петербургского политехнического университета Петра Великого.*
195251, Россия, г. Санкт-Петербург, Политехническая ул., 29
yberdnikov1947@gmail.com
ORCID: 0000-0003-0309-5917

**ИВАНИЩЕВ Дмитрий Александрович** – *кандидат физико-математических наук, старший научный сотрудник Высшей школы фундаментальных физических исследований Санкт-Петербургского политехнического университета Петра Великого.*
195251, Россия, г. Санкт-Петербург, Политехническая ул., 29
ivanishchev_da@pnpi.nrcki.ru
ORCID: 0000-0003-3298-3702

**КОТОВ Дмитрий Олегович** – *кандидат физико-математических наук, доцент Высшей школы фундаментальных физических исследований Санкт-Петербургского политехнического университета Петра Великого.*
195251, Россия, г. Санкт-Петербург, Политехническая ул., 29
Dmitriy.kotov@gmail.com
ORCID: 0000-0002-3395-0454

**МАЛАЕВ Михаил Владимирович** – *кандидат физико-математических наук, старший научный сотрудник Высшей школы фундаментальных физических исследований Санкт-Петербургского политехнического университета Петра Великого.*
195251, Россия, г. Санкт-Петербург, Политехническая ул., 29
Mmalayev@gmail.com
ORCID: 0009-0001-9974-0169

**РЯБОВ Андрей Юрьевич** – *аспирант Петербургского института ядерной физики имени Б. П. Константинова НИЦ «Курчатовский институт».*
188300, Россия, Ленинградская область, г. Гатчина, микрорайон Орлова Роща, 1
andrei.riabov@cern.ch
ORCID: 0009-0007-9874-9819

*Received 16.02.2025. Approved after reviewing 19.02.2025. Accepted 19.02.2025.*
*Статья поступила в редакцию 16.02.2025. Одобрена после рецензирования 19.02.2025. Принята 19.02.2025.*

© Peter the Great St. Petersburg Polytechnic University, 2025